Electronic Properties of Free and Coordinating Polythioether Macrocycles. A Spectroscopic and Computational Analysis

Marcus C. Durrant,[a,*] **Raymond L. Richards**[a] **and Steven Firth**[b]
[a] *AFRC IPSR Nitrogen Fixation Laboratory, University of Sussex, Brighton, UK, BN1 9RQ*
[b] *School of Chemistry and Molecular Sciences, University of Sussex, Brighton, UK, BN1 9QJ*

Helium I photoelectron spectra of the polysulfur macrocycles 1,4,7-trithiacyclodecane ([10]aneS$_3$), 1,4,7,10-tetrathiacyclododecane ([12]aneS$_4$), 1,4,8,11-tetrathiacyclotetradecane ([14]aneS$_4$), 1,5,9,13-tetrathiacyclohexadecane ([16]aneS$_4$), 3,3,7,7,11,11,15,15-octamethyl-1,5,9,13-tetrathiacyclohexadecane (Me$_8$[16]aneS$_4$) and 1,4,7,10,13,16-hexathiacyclooctadecane ([18]aneS$_6$) are reported and correlated with the results of semi-empirical molecular orbital (MO) calculations. Where available, published X-ray crystallographic data have been used to provide input geometries for the MO calculations; in addition, alternative low energy conformations have been generated by molecular mechanics. In order to probe the effects on the electronic properties of the macrocycles of changes in conformation resulting from coordination to a metal centre, MO calculations have also been carried out on conformations of [9]aneS$_3$, [12]aneS$_4$, [14]aneS$_4$ and [16]aneS$_4$ taken from X-ray structures of their metal complexes. The energy required to transform the macrocycles from their free conformations is found to be reasonably small compared to typical metal–thioether bond energies. [14]aneS$_4$ and [16]aneS$_4$ both exhibit a number of different η^4-chelating conformations of similar energies and electronic properties.

The study of metal–thioether coordination chemistry has been greatly facilitated in recent years by the use of polysulfur macrocycles as chelating ligands for an extensive range of metals.[1] However, it has become apparent that these compounds differ from other well-known classes of macrocycle in a number of important aspects. For example, unlike polyamines and crown ethers, solvent effects make a relatively minor contribution to the overall macrocyclic chelate effect of cyclic polythioether ligands, and the main contributions come rather from the differences in translational and configurational entropy in going from a set of independent thioether ligands *via* an open-chain polythioether to a macrocyclic ligand.[2] Furthermore, it is now well established by X-ray crystallography that in the solid state, in the absence of other structural constraints the sulfur atoms prefer to take up exodentate positions in the free macrocycles.[1] Wolf *et al.*[3] have discussed this phenomenon in terms of the overall electron–electron repulsion between sulfur atoms and the greater stability of gauche C–C–S–C linkages compared to their first-row analogues. If similar effects operate in solution, then to chelate to a single metal centre the macrocycle must first invert to an endodentate conformation, and the resulting energy requirement (the inversion enthalpy, ΔH_i), works against the entropy term responsible for the macrocyclic effect. This is illustrated schematically for [14]aneS$_4$ in Scheme 1. Although this problem has been revealed by crystallography, structural studies alone cannot gauge its importance, since they give no measure of the magnitude of ΔH_i. A large value of ΔH_i would imply a fairly rigid exodentate macrocycle, which could chelate only weakly to a single metal centre. On the other hand, if ΔH_i is small a large number of conformers would be thermodynamically accessible at room temperature, including the endodentate geometries required for chelation. Study of the detailed electronic properties of these molecules is thus of considerable interest, since it allows estimation of ΔH_i and related properties of relevance to their coordination chemistry.

To date, a single report by Setzer *et al.*[4] has dealt with the photoelectron spectra of a number of mesocycles of up to 10 atoms, containing two or three sulfur atoms, including [9]aneS$_3$. We now report photoelectron data for six macrocycles containing up to six sulfur atoms, all of which have found use as ligands, along with a computational analysis of the macrocycles' geometries and electronic properties using published X-ray data, molecular mechanics calculations using the MM2 and Tripos force fields and semi-empirical molecular orbital (modified neglect of diatomic overlap, MNDO) calculations. We have extended the computational analysis to include a number of the macrocycles in their coordinated geometries.

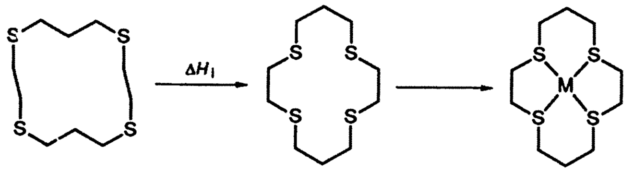

Scheme 1

Results and Discussion

In simple monothioethers, the first ionisation is from an essentially non-bonding orbital, perpendicular to the C–S–C plane and related closely to an atomic sulfur p-orbital, hence referred to as a p-type lone pair.[5] The second ionisation is from an in-plane orbital, again centred on sulfur but containing some s character and therefore commonly referred to as an s-type lone pair (in fact this orbital has some C–S bonding character). These two orbitals are primarily responsible for electron donation to the metal in thioether complexes. In the polythioethers studied here, the equivalent orbitals are not centred on individual sulfur atoms but rather delocalised over some or all of the sulfurs. For convenience we shall designate these two sets of orbitals as p-type and s-type non-bonding.

The photoelectron spectra of [18]aneS$_6$ and [16]aneS$_4$, which are typical of all the compounds studied, are shown in Fig. 1. The ionisations from the p-type sulfur non-bonding orbitals are well separated from the rest of the spectrum, giving either a broad single band or, in some cases, a doublet. The onset of the ionisations from the s-type non-bonding orbitals is distinct, but these bands then merge with those from the C–S

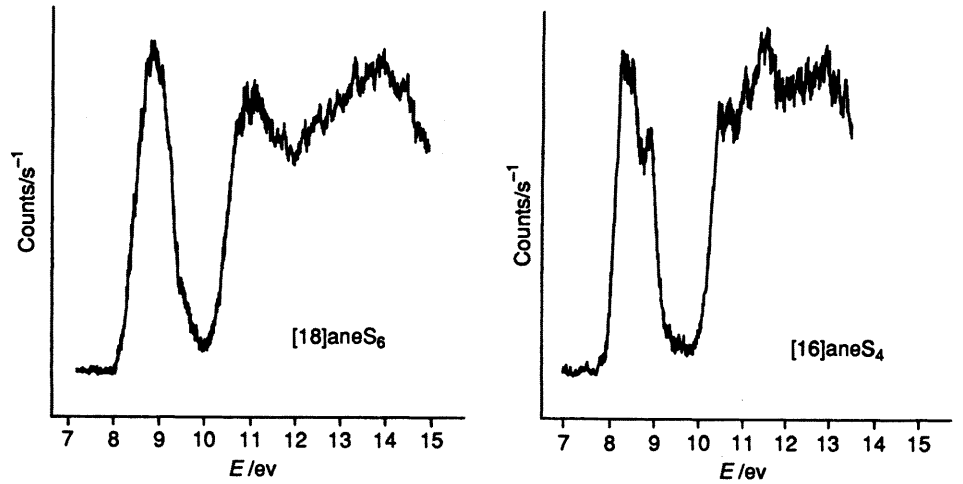

Fig. 1 Photoelectron spectra of [18]aneS$_6$ and [16]aneS$_4$

Table 1 Photoelectron data for sulfur macrocycles (eV)

	p-Type non-bonding			s-Type non-bonding
Macrocycle	Onset	Maxima	End	Onset
[9]aneS$_3$ [a]	8.16	8.44, 8.93	9.19	10.22
[10]aneS$_3$	8.03	8.41, 8.83	9.10	10.12
[12]aneS$_4$	8.44	8.68	9.19	10.25
[14]aneS$_4$	8.04	8.48	9.10	10.19
[16]aneS$_4$	8.08	8.35, 8.87	9.08	10.15
Me$_8$[16]aneS$_4$	7.76	8.20	8.65	9.67
[18]aneS$_4$	8.33	8.86	9.33	10.32

[a] Values identical to ref. 4 within the resolution limits.

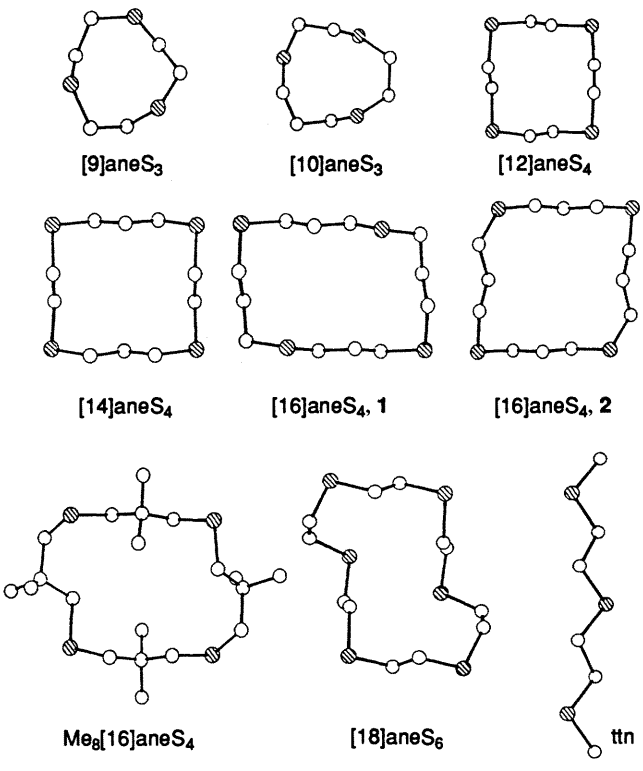

Fig. 2 Input geometries for the MNDO calculations. The geometries of [9]aneS$_3$ (ref. 9), [12]aneS$_4$ (ref. 15), [14]aneS$_4$ (ref. 14) and [18]aneS$_6$ (ref. 3) were taken from published crystallographic data; the other geometries were generated using SYBYL.

and C–C bonding orbitals to give a continuum at higher energies. The spectroscopic data are summarised in Table 1.

As an aid to interpreting the photoelectron spectra, MNDO calculations were performed on all the macrocycles studied. Where X-ray structural data were available, these were used as input geometries for the calculations. The X-ray structures of [9]aneS$_3$, [12]aneS$_4$ and [14]aneS$_4$ are in fact closely related to the solid state geometries of their parent hydrocarbons [9]ane, [12]ane and [14]ane, which are also retained in solution.[6] To the best of our knowledge, no crystal structure data are available for free [10]aneS$_3$, [16]aneS$_4$ or Me$_8$[16]aneS$_4$. These geometries were therefore extrapolated from related crystal structures and the geometries of their parent hydrocarbons by molecular mechanics using SYBYL molecular modelling software[7] (see below). The input geometries are shown in Fig. 2, and the calculated orbital energies are given in Table 2. These may be related to the experimental data by assuming Koopmans' theorem.[5]

Before considering the individual macrocycles, it is important to assess the limitations of our calculations. Although molecular mechanics calculations give conformational energies, these are at best only qualitative for molecules as complex as those studied here. The MNDO calculations give much more meaningful energies, although the error margins are still significant. The authors of MNDO[8] report a mean error in the heats of formation of a range of hydrocarbons of 25 kJ mol^{-1}, whilst the mean error for a set of sulfur compounds was 32 kJ mol^{-1}. To put these values into context, for an equilibrium between two conformers separated by a free energy difference of 10 kJ mol^{-1}, the population of the higher energy conformer would be *ca.* 1%. The best evidence for the importance of a particular conformer in the thermodynamic ensemble in this study therefore comes from comparison of the calculated orbital energies for that conformer with the photoelectron spectrum rather than the heat of formation data. This approach has been successfully applied to medium ring-size polythioethers.[4]

The photoelectron spectrum of [9]aneS$_3$ has been reported previously by Setzer *et al.*;[4] we obtained identical results. Its X-ray crystal structure[9] shows that the three sulfur atoms in [9]aneS$_3$ are equivalent by virtue of a threefold axis of symmetry, giving rise to a set of three p-type non-bonding orbitals, the first two of which are degenerate (Fig. 3). This is consistent with the doublet of relative intensity 2:1 observed in the photoelectron spectrum, suggesting that the gas phase geometry is close to that observed in the solid state.

In contrast to the photoelectron results, Blom *et al.* concluded from an electron diffraction study[10] that [9]aneS$_3$ adopts a different geometry (predominantly C_1) in the gas phase.

Table 2 Calculated non-bonding orbital energies for free sulfur macrocycles

Macrocycle	p-Type energies/eV						First s-type energy[a]/eV
[9]aneS_3	9.61	9.61	9.74	—	—	—	11.42
[10]aneS_3	9.51	9.63	9.85	—	—	—	11.39
[12]aneS_4	9.77	9.98	9.99	10.25	—	—	11.45
[14]aneS_4	9.74	9.83	9.96	10.09	—	—	11.37
[16]aneS_4, **1**	9.64	9.65	9.81	9.83	—	—	11.42
[16]aneS_4, **2**	9.66	9.73	9.77	9.87	—	—	11.43
Me_8[16]aneS_4	9.62	9.67	9.73	9.79	—	—	11.08
[18]aneS_6	9.76	9.79	9.86	9.93	10.03	10.10	11.02

[a] The higher s-type orbital energies have been omitted for simplicity.

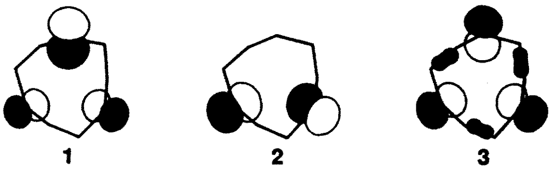

Fig. 3 Plots of the p-type non-bonding orbitals of [9]aneS_3

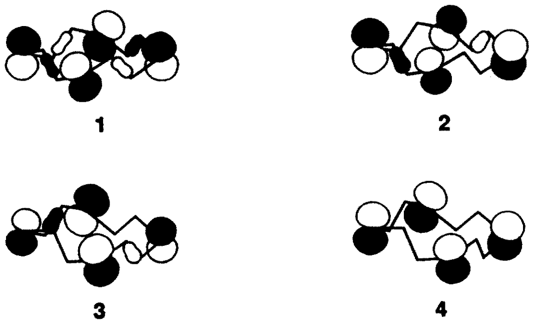

Fig. 4 Plots of the p-type non-bonding orbitals of [12]aneS_4

However, these results are not necessarily contradictory, since the higher sample temperature required for the electron diffraction experiment (*ca.* 500 K, compared to *ca.* 330 K for the photoelectron experiment) could significantly alter the population statistics of the conformational ensemble.

The photoelectron spectrum of [10]aneS_3 also gives a doublet for the p-type non-bonding ionisations, but the resolution is poorer and the relative intensities are closer to 1:1. This compound has a melting point close to room temperature, and crystallographic data are not available, though it is clear from molecular modelling studies that the inclusion of an extra CH_2 unit compared to [9]aneS_3 has a significant effect on the geometry. Lockhart and Tomkinson[11] have investigated the conformational dynamics of [10]aneS_3, whilst Setzer *et al.* have carried out a static MM2 conformational analysis by generating a set of 24 conformations derived from cyclododecane.[12] For comparison we used SYBYL's RANDOMSEARCH routine to probe the conformation of [10]aneS_3 (see Computational Details subsection). This routine uses a Monte Carlo procedure to search conformational space.[13] Although it is by no means guaranteed to find the global energy minimum within reasonable search times, the routine provides a useful sample of low energy conformers for comparison. The eight lowest energy conformations of [10]aneS_3 found were examined in detail. Five of these were reported by Setzer *et al.*, including the same energy minimum (a [1333] conformation, Fig. 2). However, these authors also reported a number of other low energy conformers not located by RANDOMSEARCH. A MNDO calculation on the minimum indicated that although the first two orbitals are not degenerate, they are still close in energy (Table 2), hence giving a reasonable fit to the photoelectron spectrum. The second lowest energy conformer, which has a related [1333] geometry and a MOPAC energy just 1.5 kJ mol^{-1} higher than the minimum, gave very similar orbital energies and is therefore probably also significantly populated.

The crystal structures of [12]aneS_4[3] and [14]aneS_4[14] show the typical exodentate conformation. The equivalence of the four sulfur atoms in these and related cases causes the sulfur p-type non-bonding orbitals to split into roughly symmetrical patterns (Table 2 and Fig. 4). This gives rise to an unresolved band in the photoelectron spectrum (*cf.* Fig. 1). The ionisation potentials for the four orbitals were estimated from the band maximum and width. For comparison with the X-ray data, 12[ane]S_4 and 14[ane]S_4 were also subjected to RANDOMSEARCH analyses. Both searches failed to locate the crystal structure geometries, but furnished a number of low energy conformers which gave comparable MOPAC energies. However, in all cases the ionisation potentials were 0.15–0.55 eV lower than for the X-ray structures. The symmetrical shapes of the first ionisation bands in the photoelectron spectra suggest that only a few closely related conformers are appreciably populated at the experimental temperatures.

[16]aneS_4 provides an interesting exception to this pattern. The p-type non-bonding ionisations are split into a doublet, suggesting that the four sulfurs are not all equivalent but rather form two pairs. To the best of our knowledge this macrocycle has not been structurally characterised, but the spectrum can be explained by reference to the parent hydrocarbon. Dale has shown that liquid [16]ane is primarily a mixture of two conformers;[6] the [16]aneS_4 analogues of these are shown in Fig. 2. Conformation **2** would be expected by extrapolation from [12]aneS_4 and [14]aneS_4, and gives a similar pattern of orbital energies, whilst **1** is closely related to the crystal structure of [12]aneS_3.[15] In this case the sulfurs are two non-equivalent pairs, giving rise to a doublet structure for the orbital energies (Table 2). The MNDO energies of the two conformers are virtually identical (**1** is just 4 kJ mol^{-1} more stable). Hence it is likely that the photoelectron spectrum of [16]aneS_4 is a composite resulting primarily from an equilibrium mixture of both conformers. RANDOMSEARCH analysis failed to locate either conformer **1** or **2**; none of the conformers found fitted the observed doublet pattern.

The incorporation of eight methyl groups into [16]aneS_4 to give Me_8[16]aneS_4 results in a return to the single broad peak for the p-type non-bonding ionisations. This is not surprising, since the extra steric requirements of the methyl groups preclude the conformation equivalent to [16]aneS_4, **1**, whereas **2** is still accessible, albeit in a rather distorted form. Me_8[16]aneS_4 has the lowest ionisation potential of all the macrocycles studied. Classically, this may be explained in terms of increased inductive electron supply to the sulfur atoms as the size of the hydrocarbon backbone is increased. The greater basicity of Me_8[16]aneS_4 over [16]aneS_4, together with the conformational differences noted above, may be reflected in differences in their coordination chemistry.

A MNDO calculation on [18]aneS_6, using the crystal data,[3] gave a reasonable fit to the observed spectrum; however, Lockhart and Tomkinson's molecular dynamics study of this

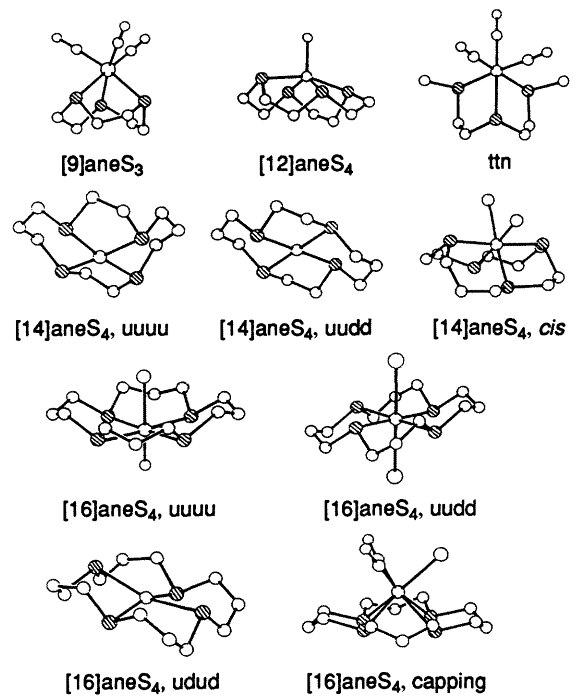

[9]aneS$_3$ [12]aneS$_4$ ttn

[14]aneS$_4$, uuuu [14]aneS$_4$, uudd [14]aneS$_4$, *cis*

[16]aneS$_4$, uuuu [16]aneS$_4$, uudd

[16]aneS$_4$, udud [16]aneS$_4$, capping

Fig. 5 Complexes used to generate endodentate geometries for the polythioethers. The formulae of the complexes are as follows; [9]aneS$_3$, [W(CO)$_3$[(9]aneS$_3$)] (ref. 16); [12]aneS$_4$, [Cu([12]aneS$_4$)(H$_2$O)] (ref. 23); ttn, [Mo(CO)$_3$(ttn)] (ref. 22); [14]aneS$_4$ uuuu, [Rh([14]aneS$_4$)]$_2^{2+}$ (ref. 17); [14]aneS$_4$ uudd, [Cu([14]aneS$_4$)]$^{2+}$ (ref. 23); [14]aneS$_4$ *cis*, [Rh([14]aneS$_4$)Cl$_2$] (ref. 18); [16]aneS$_4$ uuuu, [MoO(SH)([16]aneS$_4$)]$^+$ (ref. 19); [16]aneS$_4$ uudd, [Fe([16]aneS$_4$)I$_2$] (ref. 20); [16]aneS$_4$ udud, [Hg([16]aneS$_4$)(ClO$_4$)$_2$] (ref. 21); [16]aneS$_4$ capping, based on [MoBr(CO$_2$)(Me$_8$[16]aneS$_4$)]$^+$ (ref. 24).

Table 3 Changes in the electronic properties of sulfur macrocycles upon coordination

Species	ΔH_i/kJ mol^{-1}	ΔI_p/eV	ΔI_s/eV	ΔC/e	θ/deg
[9]aneS$_3$	0	−0.18	−0.12	+0.02	114
[12]aneS$_4$[a]	−15	−2.26	−1.96	+0.04	109
[14]aneS$_4$ uuuu	+30	−2.40	−2.10	+0.09	112
[14]aneS$_4$ uudd	−25	−2.68	−2.52	−0.04	110
[14]aneS$_4$ *cis*	0	−2.79	−2.57	+0.04	119
[16]aneS$_4$ uuuu	+10	−1.83	−1.16	+0.21	125
[16]aneS$_4$ uudd	−20	−1.97	−1.61	+0.06	115
[16]aneS$_4$ udud	+35	−1.47	−1.15	−0.03	100
[16]aneS$_4$ capping	+25	−2.65	−2.71	+0.23	121
ttn	+25	−0.78	−0.85	+0.16	118

[a] Values calculated for the idealised complex geometry (see text).

macrocycle[11] showed that it is much more flexible than the smaller rings and probably displays very complicated conformational behaviour.

We have extended our computational study to consider the electronic properties of a number of the macrocycles in their coordinated geometries, produced by editing the published crystallographic data for their metal complexes.[16–24] The geometries considered are shown in Fig. 5, and the results are summarised in Table 3. For comparison, Table 3 also includes data for a complex of an acyclic polythioether, 2,5,8-trithianonane (ttn).[22] The geometry of free ttn is unknown, but one would intuitively expect the linear conformer shown in Fig. 2 to correspond to the global energy minimum. A RANDOMSEARCH analysis of ttn was carried out, and the six lowest energy conformations found were used for MNDO calculations; the linear conformation was located and indeed had the lowest MNDO energy (though only the second lowest TRIPOS energy).

The inversion enthalpy ΔH_i required to go from a free polythioether to a given chelating conformation may be taken as the difference in heats of formation of the two conformations. As mentioned above, the error in these calculations may be up to 30 kJ mol^{-1}. Preliminary calculations on [14]aneS$_4$ showed that although the absolute values of the heats of formation obtained from single point calculations were significantly higher than those obtained after full geometry optimisation, the differences largely cancelled out in calculating ΔH_i provided that the bond lengths were consistent within the geometries being compared (*e.g.* when comparing X-ray structures with calculated structures). In view of the large increase in computer time required for geometry optimisation, plus the fact that the optimisation failed to converge for some conformers, all subsequent calculations were single point only.

In addition to ΔH_i values, Table 3 includes a number of parameters which characterise the availability of the sulfur non-bonding orbitals for bonding to a metal. ΔI_p and ΔI_s are the net destabilisations of the p-type and s-type sulfur non-bonding orbital sets respectively, given by the difference between the total energies of each set of orbitals in the free and bound geometries. The p-type and s-type orbitals are free to mix upon coordination, and the contribution made by each to the resulting σ-bonding orbital is indicated by the tilt angle θ between the bisector of the CSC angle and the metal–sulfur bond. The closer this angle is to 90°, the greater the contribution of the p-type non-bonding orbitals to the σ-bonding orbitals. Finally, ΔC is the total change in Mulliken charge on all the sulfur atoms on going from the free to the coordinated geometry.

As shown in Table 3, the inversion enthalpy of [9]aneS$_3$ is close to zero. This is expected, since the small ring size forces the sulfur atoms into an endocyclic conformation which requires very little rearrangement for chelation to a metal.[1] [9]aneS$_3$ is a popular ligand; more than 30 of its metal complexes have been reported to date. In contrast, the only complex of [12]aneS$_4$ which has been structurally characterised so far[23] is [Cu([12]aneS$_4$)(H$_2$O)](ClO$_4$)$_2$. An initial calculation on the macrocyclic fragment of this complex gave a very high inversion enthalpy (345 kJ mol^{-1}). However, there were difficulties with the refinement of this structure,[23] resulting in some unrealistic dimensions (the C–S–C bond angles, for example, varied from 79° to 127°). We tried using SYBYL to generate an idealised geometry from the crystallographic data (see Computational Details subsection). This approach gave much more reasonable dimensions (*e.g.* C–S–C angles 101.2–104.8°). The value of ΔH_i was now actually negative (Table 3), suggesting that if anything the structure was a little too ideal. Nevertheless, this result implies that the dearth of complexes of [12]aneS$_4$ has more to do with the poor match in ligand–metal geometry than a high inversion enthalpy.

The larger macrocycles [14]aneS$_4$ and [16]aneS$_4$ can chelate through all four sulfur atoms in a variety of ways, as shown in Fig. 5. [14]aneS$_4$ is known to coordinate in two equatorial conformations and one *cis* conformation, whilst three equatorial conformations have been demonstrated for [16]aneS$_4$, termed 'all-up' (*syn*), 'up-up-down-down' (*anti*), and 'up-down-up-down'. We abbreviate these as uuuu, uudd, and udud respectively. In addition, we have recently observed[24] a capping geometry for Me$_8$[16]aneS$_4$ in the complex cation [MoBr(CO)$_2$(Me$_8$[16]aneS$_4$)]$^+$. For the sake of comparison, we have used our X-ray data for this complex to generate the equivalent geometry for [16]aneS$_4$ by editing out the methyl groups.

The results show similar trends for [14]aneS$_4$ and [16]aneS$_4$. In both cases, the uudd geometry is calculated to be *more* stable than the free exodentate conformation, a result which, at first sight, is at odds with the conclusions of the crystallographic studies mentioned above. The most likely explanation is that

MNDO overestimates the steric repulsion in the hydrocarbon chains of the exodentate conformers compared to the sulfur 'lone pair' repulsion in the endodentate conformers, consistent with the known limitations of this method.[8] The values of ΔH_i for these conformers are within MNDO's likely margin of error. Nevertheless, we can say that the inversion enthalpies for all the coordinated geometries of [14]aneS$_4$ and [16]aneS$_4$ are clearly much smaller than the enthalpy gain in forming four metal–sulfur bonds (M–S bond enthalpies are typically 200–300 kJ mol^{-1}).

For all the conformations, the switch from exodentate to endodentate conformation is marked by a destabilisation of the sulfur non-bonding orbitals, reflected in decreases in the energies of these orbitals (Table 3). The tilt angles θ vary quite widely, from 100° to 125°, the value expected for sp^3 hybridisation. This suggests that the hybridisation of the sulfurs is not critical to the metal–sulfur bonding. Nevertheless, the observation that the metal invariably lies out of the plane of the four sulfur atoms in complexes of [14]aneS$_4$ and [16]aneS$_4$ possessing the uuuu geometry[1] may result from a drive to reduce θ, which is larger for the uuuu geometries than the uudd geometries (Table 3). Overall there is net migration of electron density away from sulfur, evidenced by an increase in the Mulliken charge. For [16]aneS$_4$ the biggest effects are for the capping conformation, where the mean distance between adjacent sulfurs is only 2.99 Å, whilst the [16]aneS$_4$ udud conformer, which has the largest intersulfur distance (3.75 Å), shows the smallest effects at sulfur. However, this very distorted geometry, resulting from encapsulation of the large mercury ion, is also calculated to be the least stable.

Comparison of the more common uudd and uuuu geometries of [14]aneS$_4$ and [16]aneS$_4$, which show parallel trends, reveals subtle differences between the two. The uudd conformers suffer a slightly greater destabilisation of the sulfur non-bonding orbitals than their uuuu counterparts, whereas the latter show higher net electron loss from sulfur than do the former. There are also small yet systematic variations in θ. The overall effects of these variations on the metal–sulfur bonding are difficult to judge. Clearly there are no gross differences, and other factors beyond the scope of our calculations (*e.g.* the role of sulfur d-orbitals in back-bonding) may determine the preferred conformation in a particular complex. This is in line with the known chemistry of these complexes, where equilibria between the two geometries have been demonstrated in a number of cases.[25]

Finally, the changes in the electronic properties of the acyclic polythioether ttn upon going to the complexed geometry are of the same order as for the macrocyclic ligands. Hence apart from entropy effects and differences in physical characteristics (the macrocycles are generally moderately volatile solids, whereas their acyclic counterparts are involatile liquids), the distinctions between the two types of ligand appear to be fairly marginal.

Conclusions

It has been argued by Desper *et al.*[26] that since acyclic polythioethers demonstrate the same conformational preferences as their macrocyclic analogues, macrocycles based on ethylene sulfide units will generally be poor chelating ligands. However, our calculations indicate that in general the energies required to transform the conformations of both cyclic and acyclic polythioethers to allow chelation to a metal are unlikely to present a major hindrance to complexation. The increase in sulfur lone pair repulsion is manageable, and its contribution to ΔH_i is partially offset by reductions in steric repulsion in the hydrocarbon backbone.

Thioethers are generally relatively poor ligands, and incorporation into a macrocycle does not produce any fundamental changes. Nevertheless, provided care is taken to match the macrocycle cavity size to the metal, entropy effects should make a useful contribution to complex stability.

Experimental

Materials.—With the exception of Me$_8$[16]aneS$_4$, the macrocycles were synthesised by literature methods[27] or purchased directly from the Aldrich Chemical Co. All preparations were done under a nitrogen atmosphere using solvents purified by standard methods. *J*-Values are given in Hz.

Synthesis of Me$_8$[16]aneS$_4$.—*Preparation of* 4,8-*dithia*-2,2,6,6,10,10-*hexamethylundecane*-1,11-*diol.* Sodium (20 g, 0.87 mol) was added to ethanol (870 cm^3), followed by 2,2-dimethylpropane-1,3-dithiol[28] (58.4 g, 0.43 mol). The solution was stirred at 60 °C for 30 min, then 3-bromo-2,2-dimethylpropan-1-ol (106 cm^3, 0.86 mol) was added and the mixture boiled under reflux for 2.5 h. After cooling, hexane (1 dm^3) was added and the mixture was repeatedly filtered. The solvent was removed and the residue was heated to 180 °C under vacuum (0.001 mmHg). Upon cooling to −5 °C it solidified to a sticky, near-colourless glass (102 g, 77%), ν_{max}/cm^{-1} 3370 br (OH) and 1044 (C–O); δ_H(270 MHz; CD$_2$Cl$_2$) 0.94 [12 H, s, C(2,10)Me$_2$], 1.01 [6 H, s, C(6)Me$_2$], 2.11 (2 H, t, *J* 6.0, OH), 2.55 [4 H, s, C(5,7)H$_2$], 2.58 [4 H, s, C(3,9)H$_2$] and 3.38 [4 H, d, *J* 6.0, C(1,11)H$_2$].

4,8-*Dithia*-2,2,6,6,10,10-*hexamethyl*-1,11-*undecyl-di*(p-*toluenesulfonate*). *p*-Toluenesulfonyl chloride (74 g, 0.39 mol) was added portionwise to a solution of 4,8-dithia-2,2,6,6,10,10-hexamethylundecane-1,11-diol (60 g, 0.19 mol) in pyridine (150 cm^3) at 0 °C. The mixture was stirred at 0 °C for 60 min, then excess ice-cold sulfuric acid was added and the mixture was extracted with diethyl ether. The extract was washed with water and dried. The solvent was removed by rotary evaporation, and the residue was left under vacuum (< 1 mmHg) on the rotary evaporator at 35–40 °C for 5 h, giving the product as a viscous brown oil (100 g, 85%), ν_{max}/cm^{-1} 1360, 1185 (S=O), 969 (C–O), 841, and 667 and 553 (sulfonate); δ_H(CD$_2$Cl$_2$; Me$_4$Si) 0.93 [12 H, s, C(2,10)Me$_2$], 0.94 [6 H, s, C(6)Me$_2$], 2.44 (6 H, s, Ph*Me*), 2.45 [4 H, s, C(5,7)H$_2$], 2.47 [4 H, s, C(3,9)H$_2$], 3.80 [4 H, s, C(1,11)H$_2$], 7.37 (4 H, d, *J* 8.3, Ph) and 7.77 (4 H, d, *J* 8.3 Ph).

Preparation of 3,3,7,7,11,11,15,15-*octamethyl*-1,5,9,13-*tetrathiacyclohexadecane.* A solution of the *p*-toluenesulfonate (30.07 g, 48.7 mmol) plus 2,2-dimethylpropane-1,3-dithiol (6.64 g, 48.7 mmol) in *N*,*N*-dimethylformamide (DMF), (180 cm^3) was added dropwise to a well-stirred suspension of caesium carbonate (32 g, 98 mmol) in DMF (3.8 dm^3) at 50–60 °C over 68 h, using the apparatus described previously.[27] After the addition the mixture was stirred at 50 °C for a further 1 h, then the solvent was distilled off under vacuum. The solid residue was extracted with a mixture of hexane and water; the combined organic extract was washed with water, dried, and evaporated to dryness to give an oily slurry. This was cooled to −5 °C, shaken with cold methanol, and filtered to give the product as colourless crystals (4.2 g, 21%), whose properties were identical to those reported in the literature.[29]

Instrumentation.—IR spectra were recorded on a Perkin-Elmer 883 instrument. NMR spectra were recorded on a Jeol GSX 270 spectrometer. Photoelectron spectra were recorded on a Perkin-Elmer PS16 spectrometer with a modified high intensity lamp, and calibrated with the argon ^{2}P and iodomethane ^{2}E lines. The resolution was 20–40 meV. Solid samples were introduced into the spectrometer in a chamber located directly above the lamp, which was air-cooled. Lamp temperatures of 350 K ([9]aneS$_3$) to 450 K ([18]aneS$_6$) were required to give sufficient vapour pressure to obtain the spectra.

Computational Details.—All calculations were performed on an Evans and Sutherland ESV 10/32 workstation using SYBYL (version 5.4) molecular modelling software[7] interfaced to MOPAC (version 5.0).[30] Crystallographic coordinates were retrieved from the CSSR database at Daresbury. For consistency, all hydrogen atom positions were recalculated by SYBYL.

Molecular mechanics calculations were done using the MM2[31] and TRIPOS[32] force fields. Electrostatic terms were omitted from all the calculations; although the latter may have an important influence on conformation, the lack of reliable input data for the electrostatic expressions would make their inclusion rather arbitrary. The authors of TRIPOS found that results were superior for a wide range of molecules when electrostatic terms were neglected.[32] We assessed the accuracy of our calculations by generating models of [9]aneS_3, [12]aneS_4 and [14]aneS_4 and comparing these to the crystal structures. Both force fields gave good results but MM2 was consistently slightly better. Summaries of the observed and calculated structures have been deposited as supplementary data.* SYBYL uses the TRIPOS force field as the default for the routines used in this study, including RANDOMSEARCH. Consequently all the model structures of free macrocycles were put through a final MM2 refinement before use in the MNDO calculations. The coordinates of all the calculated structures have been deposited as supplementary data.

The default options were employed for the RANDOMSEARCH analysis of [10]aneS_3, as follows; energy cutoff 290 kJ, RMS threshold for distinguishing conformers 0.20, number of cycles 999, minimisation gradient convergence 0.005. The search took 11.3 h to find 124 unique conformations. The minimum was found 19 times; five other conformations had energies within 10 kJ of this. For ttn, [12]aneS_4 and [16]aneS_4 the following RANDOMSEARCH options were chosen; cutoff 125 kJ, RMS threshold 0.8, 999 cycles, convergence 0.008. The ttn search took 9.4 h to find 48 unique conformations; the minimum was found 9 times and 41 other conformations had energies within 10 kJ of this. The [12]aneS_4 search took 9.2 h to find 96 unique conformations; the minimum was found 30 times, and four other conformations had energies within 10 kJ. For [16]aneS_4, the 18.4 h search found 103 unique conformations, of which 18 had energies within 10 kJ of the minimum, which was found seven times. The RANDOMSEARCH options for [14]aneS_4 were as follows; cutoff 210 kJ, RMS threshold 1.2, 1999 cycles, convergence 0.010. The search took 27.8 h to find 64 unique conformations; the minimum was found 56 times, and 10 other conformations had energies within 10 kJ of this.

The TRIPOS force field was used to model the complex $[Cu([12]aneS_4)(OH_2)]^{2+}$. The water ligand was flagged as 'not interesting'. The crystallographic coordinates were taken as the starting geometry, and the following constraints were defined; Cu–S bond lengths 2.33 Å (k = 1000 kcal mol^{-1} Å^{-2}); S–Cu–S angles 86.9° (k = 0.08 kcal mol^{-1} deg^{-2}). The bond lengths and angles are the average values found in the crystal structure; the force constants were chosen by trial and error, such that upon energy minimisation the anomalies in the geometry of the macrocyclic ligand were corrected whilst keeping the perturbation of the coordination sphere of the copper atom to a minimum (mean Cu–S length and S–Cu–S angle in the idealised structure 2.33 Å and 86.4° respectively). A comparison of the observed and calculated structures is included in the supplementary data.

Acknowledgements

We would like to acknowledge the use of the SERC funded Chemical Databank Service at Daresbury for part of the work described in this paper.

References

1 S. R. Cooper and S. C. Rawle, *Struct. Bonding* (*Berlin*), 1990, **72**, 1.
2 G. F. Smith and D. W. Margerum, *J. Chem. Soc., Chem. Commun.*, 1975, 807.
3 R. E. Wolf, J. R. Hartman, J. M. E. Storey, B. M. Foxman and S. R. Cooper, *J. Am. Chem. Soc.*, 1987, **109**, 4328.
4 W. N. Setzer, B. R. Coleman, G. S. Wilson and R. S. Glass, *Tetrahedron*, 1981, **37**, 2743.
5 D. W. Turner, C. Baker, A. D. Baker and C. R. Brundle, *Molecular Photoelectron Spectroscopy*, Wiley, London, 1970.
6 J. Dale, *Acta Chem. Scand.*, 1973, **27**, 1115.
7 SYBYL 5.4, Tripos Associates, 1699 S. Hanley Road, Suite 303, St. Louis, MO 63144, USA.
8 M. J. S. Dewar and W. Thiel, *J. Am. Chem. Soc.*, 1977, **99**, 4899; M. J. S. Dewar and C. H. Reynolds, *J. Comput. Chem.*, 1986, **7**, 140.
9 R. S. Glass, G. S. Wilson and W. N. Setzer, *J. Am. Chem. Soc.*, 1980, **102**, 5068.
10 R. Blom, D. W. H. Rankin, H. E. Robertson, M. Schröder and A. Taylor, *J. Chem. Soc., Perkin Trans. 2*, 1991, 773.
11 J. C. Lockhart and N. P. Tomkinson, *J. Chem. Soc., Perkin Trans. 2*, 1992, 533.
12 W. N. Setzer, Q. Guo and E. J. Meehan, *Heteroatom Chemistry*, 1990, **1**, 425.
13 For a discussion of random conformational searching, see M. Saunders, K. N. Houk, Y. D. Wu, W. C. Still, M. Lipton, G. Chang and W. C. Guida, *J. Am. Chem. Soc.*, 1990, **112**, 1419; D. M. Ferguson and D. J. Raber, *J. Am. Chem. Soc.*, 1989, **111**, 4371.
14 R. E. DeSimone and M. D. Glick, *J. Am. Chem. Soc.*, 1976, **98**, 762.
15 S. C. Rawle, G. A. Admans and S. R. Cooper, *J. Chem. Soc., Dalton Trans.*, 1988, 93.
16 H.-J. Kim, Y. Do, H. W. Lee, J. H. Jeong and Y. S. Sohn, *Bull. Korean Chem. Soc.*, 1991, **12**, 257. We have also obtained the crystal structure of this compound, with essentially identical results (M. C. Durrant, B. Goerdt, D. L. Hughes and R. L. Richards, unpublished work).
17 T. Yoshida, T. Ueda, T. Adachi, K. Yamamoto and T. Higuchi, *J. Chem. Soc., Chem. Commun.*, 1985, 1137.
18 T. F. Lai and C. K. Poon, *J. Chem. Soc., Dalton Trans.*, 1982, 1465.
19 R. E. DeSimone and M. D. Glick, *Inorg. Chem.*, 1978, **17**, 3474.
20 A. Hills, D. L. Hughes, M. Jimenez-Tenorio, G. J. Leigh, A. Houlton and J. Silver, *J. Chem. Soc., Chem. Commun.*, 1989, 1774.
21 T. E. Jones, L. S. W. L. Sokol, D. B. Rorabacher and M. D. Glick, *J. Chem. Soc., Chem. Commun.*, 1979, 140.
22 M. T. Ashby, J. H. Enemark, D. L. Lichtenberger and R. B. Ortega, *Inorg. Chem.*, 1986, **25**, 3154.
23 V. B. Pett, L. L. Diaddario, E. R. Dockal, P. W. Corfield, C. Ceccarelli, M. D. Glick, L. A. Ochrymowycz and D. B. Rorabacher, *Inorg. Chem.*, 1983, **22**, 3661.
24 M. C. Durrant, D. L. Hughes, R. L. Richards, P. K. Baker and S. D. Harris, *J. Chem. Soc., Dalton Trans.*, 1992, 3399.
25 J. M. Desper and S. H. Gellman, *J. Am. Chem. Soc.*, 1991, **113**, 704; N. Herron, O. W. Howarth and P. Moore, *Inorg. Chim. Acta*, 1976, **20**, L43; T. Adachi, M. C. Durrant, D. L. Hughes, C. J. Pickett, R. L. Richards, J. Talarmin and T. Yoshida, *J. Chem. Soc., Chem. Commun.*, 1992, 1464.
26 J. M. Desper, D. R. Powell and S. H. Gellman, *J. Am. Chem. Soc.*, 1990, **112**, 4321.
27 M. C. Durrant and R. L. Richards, *Chem. Ind.* (*London*), 1991, 474.
28 E. L. Eliel, V. S. Rao, S. Smith and R. O. Hutchins, *J. Org. Chem.*, 1975, **40**, 524.
29 T. Yoshida, T. Adachi, T. Ueda, M. Watanabe, M. Kaminaka and T. Higuchi, *Angew. Chem. Int. Ed. Engl.*, 1987, **26**, 1171.
30 J. J. P. Stewart, *QCPE*, Program No. 455, Frank J. Seiler Research Laboratory, US Air Force Academy, Colorado Springs, CO 80840, USA.
31 N. L. Allinger and Y. H. Yuh, *QCPE*, Program No. 395, Quantum Chemistry Program Exchange, Indiana University Chemistry Department, Bloomington, IN, USA.
32 M. Clark, R. D. Cramer and N. V. Opdenbosch, *J. Comput. Chem.*, 1989, **10**, 982.

Paper 2/05548A
Received 19th *October* 1992
Accepted 7th *December* 1992

---

* Supp. Pub. No. 56924, 17 pp. For details of the deposition scheme see 'Instruction for Authors,' *J. Chem. Soc., Perkin Trans. 2*, 1993, issue 1.